# Magnetization and resistivity measurements of the first-order vortex phase transition in $(La_{1-x}Sr_x)_2CuO_4$

T. Sasagawa
*Department of Superconductivity, University of Tokyo, 7-3-1 Hongo, Bunkyo-ku, Tokyo 113-8656, Japan and Laboratory for Advanced Materials, Stanford University, Stanford, California 94305*

Y. Togawa and J. Shimoyama
*Department of Superconductivity, University of Tokyo, 7-3-1 Hongo, Bunkyo-ku, Tokyo 113-8656, Japan*

A. Kapitulnik
*Laboratory for Advanced Materials, Stanford University, Stanford, California 94305*

K. Kitazawa and K. Kishio
*Department of Superconductivity, University of Tokyo, 7-3-1 Hongo, Bunkyo-ku, Tokyo 113-8656, Japan*
(Received 20 July 1999)

We report magnetization and resistivity measurements of the first-order vortex lattice phase transition (FOT) in single crystals of $(La_{1-x}Sr_x)_2CuO_4$ ($0.046 \leqslant x \leqslant 0.077$). Through the comparison of the present results with $YBa_2Cu_3O_y$ and $Bi_2Sr_2CaCu_2O_y$, we show that the key parameters for the FOT are the anisotropy factor, the distance between superconducting layers, and the critical temperature. This is reflected in the observation of systematic changes, similar trends, and universal behaviors in the signatures of the FOT when the particular normalization is applied to the scales. Based on the results, the mechanism of the FOT in high-temperature superconductors is discussed.

## I. INTRODUCTION

The mixed state in the high-temperature superconductors (HTSC's) has shown the richness of novel physics. The most striking aspect is the variety of vortex states, and therefore phase transitions between different vortex states have been experimentally and theoretically explored.[1] One of the distinct phase boundaries in the field-temperature ($H$-$T$) phase diagram is the first-order transition (FOT) line, which separates the vortex solid (lattice) state and the vortex fluid (liquid or gas) state.

The FOT has been extensively studied in $YBa_2Cu_3O_y$ (Y123) (Ref. 2–11) and $Bi_2Sr_2CaCu_2O_y$ (Bi2212) (Refs. 12–22) crystals, and the phenomenon has been established in both of the systems. However, the details of the underlying mechanism of this transition are still unclear. Two competing scenarios for the FOT are a *melting* transition[23] and a *sublimation* transition.[24] The former is the transition of the vortex solid into a liquid, in which the triangular vortex lattice loses its shear modulus. The latter is the transition into a vortex gas, where the melting is accompanied by the simultaneous decoupling of the vortex lines into pancake vortices.

$(La_{1-x}Sr_x)_2CuO_4$ (La214) system is one of the well studied prototype HTSC's. The La214 system, however, has made only a small contribution to the phase transition issue in the vortex matter. In fact, only a few reports on magnetization measurements[25,26] have shown the existence of the FOT in this system. As has been recognized, the strong anisotropy of the layered HTSC materials plays a crucial role for the vortex lattice phase transition. In this context, examining the FOT more systematically in materials with various degrees of anisotropy should be enlightening as to the nature of the phenomenon. We thought that the La214 system would be the ideal compounds for this end. First of all, the La214 system fills the gap between the rather three-dimensional Y123 system and the two-dimensional Bi2212 system. In fact, the value of anisotropy factor $\gamma^2$ ($\equiv m_c^*/m_{ab}^*$) for La214 system lies intermediate ($\gamma^2 = 2 \times 10^2 - 4 \times 10^3$) (Refs. 27–29) between those for Y123 ($\gamma^2 = 25 - 1 \times 10^2$) (Ref. 30) and Bi2212 ($\gamma^2 = 3 \times 10^3 - 3 \times 10^4$) (Ref. 31) systems. In addition, the fact that the value of $\gamma^2$ can be easily and systematically controlled with Sr composition $x$ in the La214 compounds makes this system experimentally attractive. In other words, the La214 system is the sole candidate so far to fill the gap between Y123 and Bi2212 with the advantages of covering a wide range of anisotropy and of the availability of a series of single crystals.

In this paper, we examined the first-order vortex lattice phase transition in the La214 system by magnetization and resistivity measurements. For the reasons given above, comparisons were made throughout the paper between the results obtained in the La214 system and those reported in the literature for the Y123 and Bi2212 systems.

## II. SAMPLE PREPARATION AND EXPERIMENTAL PROCEDURE

Because the first-order vortex lattice phase transition has been observed only in very clean samples of Y123 and Bi2212, $(La_{1-x}Sr_x)_2CuO_{4-\delta}$ (La214) single crystals were prepared by the traveling-solvent-floating-zone (TSFZ) method[28] to avoid impurity contamination. In addition, a careful post-annealing procedure was performed in order to

 

TABLE I. Characteristic parameters for $(La_{1-x}Sr_x)_2CuO_4$, $YBa_2Cu_3O_y$ (Ref. 4), $Bi_2Sr_2CaCu_2O_y$ (Ref. 16), and $\kappa$-(BEDT-TTF)$_2$Cu[N(CN)$_2$]Br (Ref. 39) crystals.

| Sample | $T_c$/K | $\Delta T_c$/K | $s$/ Å | $\rho_{ab}$(50 K)/m$\Omega$ | $\rho_c$(50 K)/m$\Omega$ | $\gamma^2=\rho_c/\rho_{ab}$ |
|---|---|---|---|---|---|---|
| $(La_{1-x}Sr_x)_2CuO_4$ ($x=0.046$) | 25.6 | 0.4 | 6.6 | 0.65 | 1900 | 2900 |
| (0.068) | 34.9 | 0.9 | 6.6 | 0.32 | 280 | 880 |
| (0.077) | 36.6 | 0.3 | 6.6 | 0.16 | 66 | 410 |
| $YBa_2Cu_3O_y$ (Ref. 4) | 92.9 | 0.3 | 11.7 | | | (50) |
| $Bi_2Sr_2CaCu_2O_y$ (Ref. 16) | 78.3 | 1.1 | 15.4 | | | (10000) |
| $\kappa$-(BEDT-TTF)$_2$Cu[N(CN)$_2$]Br (Ref. 39) | 11.3 | 1.0 | 15.0 | | | (2000) |

remove oxygen defects ($\delta\sim 0$).[25,34]

La214 crystals with nominal Sr compositions of $x=0.05$, 0.075, and 0.080 were grown. Crystal orientations were determined by an x-ray back-reflection Laue technique. Rectangular crystals with typical dimensions of $2.0\times 0.7\times 3.0$ mm$^3$, having long edges along $a(b)$ axis ($ab$ crystal) and $c$ axis ($c$ crystal), were sectioned from grown rods by a diamond wheel saw. The Sr contents $x$ were determined by electron-probe-micro analysis (EPMA; JEOL JXA-8600) to be 0.046, 0.068, and 0.077, respectively. These crystals were sealed in quartz ampoules under controlled initial oxygen pressures ($P_{O2}=100$, 600, and 700 torr, respectively, for the $x=0.046$, 0.068, and 0.077 crystals), and annealed at 900 °C for 10 days, followed by rapid quenching to room temperature.

In-plane (out-of-plane) resistive component $\rho_{ab}(\rho_c)$ was measured on $ab$ crystals ($c$ crystals) by the ac four-probe technique using a Quantum Design PPMS-6000. The critical temperature $T_c$ (midpoint) with the transition width $\Delta T_c(10-90\,\%)$ was determined from the resistivity measurements in zero magnetic field. The anisotropy factor $\gamma^2$ was defined as the ratio of the out-of-plane to in-plane resistive components ($\rho_c/\rho_{ab}$) at 50 K. These parameters together with $s$, the distance between superconducting planes, are summarized in Table I. Resistivity in a magnetic field applied at various angles with respect to the $c$ axis was measured on $ab$ crystals with a typical current density of $J=2.1$ A/cm$^2$ along the $a(b)$ axis. To minimize the demagnetization effect, magnetization was measured on $c$ crystals with external magnetic fields of up to 50 kOe applied parallel to the $c$ axis. Magnetization measurements were performed using a SQUID magnetometer (Quantum Design MPMS).

Before proceeding to Sec. III, it should be noted here that the abovementioned careful heat treatment turned out to be quite effective in improving the quality of La214 single crystals. The effects of the post-annealing procedure are demonstrated in Fig. 1, which shows the shielding (ZFC: zero-field cooled) and Meissner (FC: field-cooled) curves of the $x=0.046$ crystal before and after heat treatments. Careful post-annealing procedure is found to result in the sharp superconducting transition and the enhancement of the Meissner fraction, indicating that the treated crystal is less disordered and very clean.

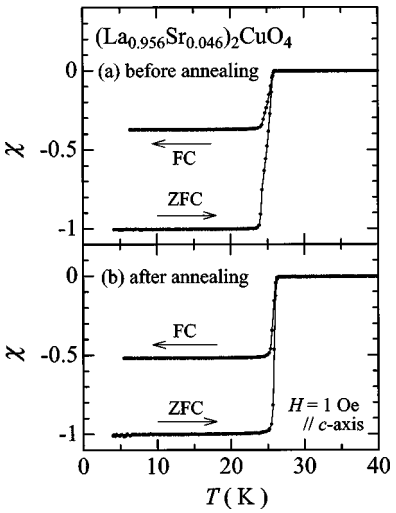


FIG. 1. Temperature dependence of the magnetic susceptibility in ZFC (zero-field-cooled) and FC (field-cooled) for the $(La_{0.954}Sr_{0.046})_2CuO_4$ single crystal before and after heat treatments. Careful post annealing procedure resulted in sharp superconducting transition and enhancement of the Meissner fraction.

## III. RESULTS

### A. Magnetization measurements

Shown in Fig. 2 are the $M$-$H$ curves for the $x=0.046$ crystal at several temperatures. A magnetization anomaly, which we associate with the first-order transition (FOT) of the vortex lattice, is observed in each $M$-$H$ curve above the

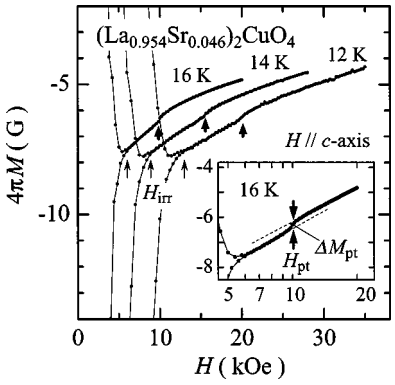


FIG. 2. Magnetization curves for the $(La_{0.954}Sr_{0.046})_2CuO_4$ single crystal as a function of magnetic field at various temperatures. The thick and thin arrows indicate the phase transition field $H_{pt}(T)$ and the irreversibility fields $H_{irr}(T)$, respectively. Inset: Semilogarithmic plot of the $M$-$H$ curve at 16 K. The magnitude of $\Delta M_{pt}$ has been defined as difference between the two log $H$-linear parts at the phase transition field $H_{pt}$.

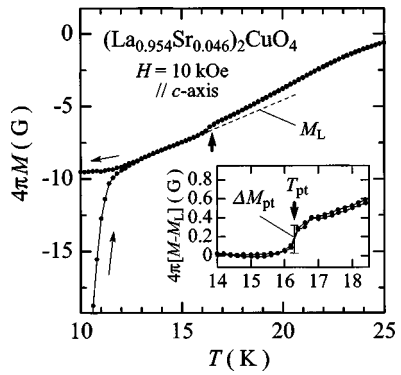


FIG. 3. Temperature dependence of magnetization curves for the $(La_{0.954}Sr_{0.046})_2CuO_4$ single crystal. Inset: A linear extrapolation of low-temperature reversible magnetization $M_L$ (dotted line in the main panel) is subtracted from the magnetization to determine the magnetization change $\Delta M_{pt}$.

irreversibility field $H_{irr}$ which is defined as a field in which the magnetization hysteresis $4\pi\Delta M$ becomes smaller than $5\times10^{-2}$ G.

The phase transition observed in La214 seems to be not as sharp as that seen in the micro-Hall probe measurements on Bi2212.[13,14] It has been thought that the observation of a clear phase transition anomaly is not easy in the La214 system due to the defective nature of this compound, which is rather inherent to the system. This is due to the fact that the charge reservoir layer in this system, La(Sr)-O layer, is defective at the immediate $CuO_2$ layer which contributes to the manifestation of superconductivity. Both in Bi2212 and Y123 systems, in contrast, the defective layer in the charge reservoir region is located away from the $CuO_2$ layer by the intervening layer of SrO and BaO, respectively. In other words, superconducting properties of the La214 system are very sensitive to the inhomogeneity of the local Sr distribution in the La(Sr)-O layers. Therefore, the La214 system can easily become dirty.

However, judging from the sharp superconducting transition as shown in Fig. 1, we think that the present La214 crystals are not as *dirty* as has been believed. It is found that the apparently dull transition seen in the main panel of Fig. 2 is attributable to the effect of the field dependence of reversible magnetization. Following either the London model[32] or a modified model for HTSC,[33] the reversible magnetization depends logarithmically on $H$. To check this magnetization behavior, the $M$-$H$ curve is plotted on a semi logarithmic scale as shown in the inset of Fig. 2. Magnetization above $H_{irr}$ is, in fact, linear in $\log H$, and the jump in the magnetization is clearly recognized at the phase transition field $H_{pt}$ in this plot. Then, the magnetization change $\Delta M_{pt}$ at the FOT has been defined as difference between the two $\log H$-linear parts at $H_{pt}$.

It is noted that $\Delta M_{pt}>0$ at the phase transition, indicating that the vortex density increases when the vortex state changes from solid into fluid. This is the same behavior observed in Y123 (Refs. 5–7) and Bi2212 (Refs. 12–17), and has been regarded as thermodynamic evidence of the first-order phase transition of the vortex system.

In the temperature-scan measurements, a similar magnetization anomaly is observed (Fig. 3), and the obtained phase

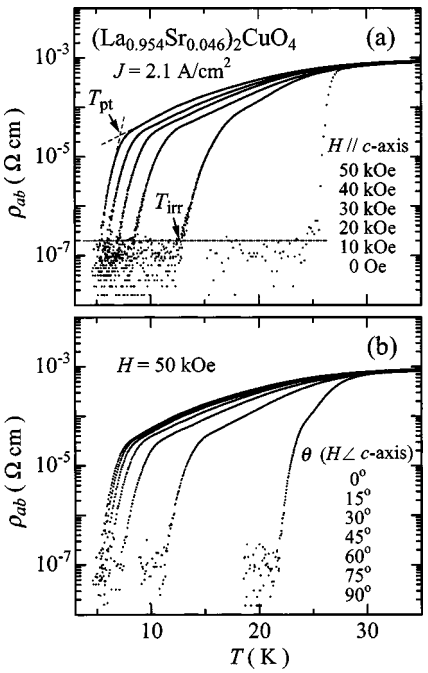


FIG. 4. Temperature dependence of the $ab$-plane resistivity $\rho_{ab}$ in the $(La_{0.954}Sr_{0.046})_2CuO_4$ single crystal (a) under various fields applied parallel to the crystal $c$ axis, and (b) as a function of the angle $\theta$ between the $c$ axis and the field ($H=50$ kOe).

transition temperature $T_{pt}$ was in good agreement with the independently determined phase transition field $H_{pt}$ from the $M$-$H$ measurements, e.g., $T_{pt}\sim16$ K at $H=10$ kOe agreed with $H_{pt}\sim10$ kOe at $T=16$ K. In order to determine the magnitude of $\Delta M_{pt}$, a linear extrapolation of low-temperature reversible magnetization $M_L$ (dotted line in Fig. 3) is subtracted from the magnetization, as shown in the inset of Fig. 3. The obtained value of $\Delta M_{pt}$ agreed well with those from the $M$-$H$ measurements. It is interesting to note that the slope of the temperature dependence of magnetization above $T_{pt}$ is steeper than that below $T_{pt}$, consistent with the observation in the Y123 system.[5]

The FOT was also observed in the $x=0.068$ and 0.077 crystals. The FOT is reported to terminate in the low-temperature and high-field region in Y123 (Refs. 4,10,35,36) and Bi2212 (Ref. 13,14,16,17). However, for all the La214 samples examined, such disappearance of the FOT at higher fields was not observed within the field range measured in this study. In Sec. IV C, we will discuss the magnitude of the magnetization change and the associated entropy change at the vortex transition with reference to the results for the Y123 and Bi2212 compounds.

### B. Resistivity measurements

The magnetization anomaly which we attributed to the FOT was observed in the reversible magnetization ($H>H_{irr}$). Since this result suggested that the FOT lay within the dissipative region, the corresponding resistivity anomaly was expected to be similarly observed as has been reported in Y123 (Refs. 2–5) and Bi2212 (Refs. 16,17). Therefore the temperature dependence of $ab$-plane resistivity $\rho_{ab}$ in magnetic fields was measured in detail.

Figure 4(a) shows the $\rho_{ab}(T)$ curves in the $x=0.046$ crys-

tal in various magnetic fields parallel to the $c$ axis. In addition to the significant resistivity broadening in the field, a new feature is evident in this figure. At around $\rho_{ab}=10^{-5}\sim10^{-4}\Omega$ cm, the slope of $\rho_{ab}(T)$ is seen to change abruptly, and the resistivity shows a sharp drop below the point which is defined as $T_{pt}$. This is the first time this resistive behavior in a field has been observed in the present La214 system.

Although the resistive kink in a field in La214 is reminiscent of the signature of the FOT in Y123 and Bi2212, other interpretations cannot be ruled out at this stage for the La214 crystals. Since the La214 compounds undergo a tetragonal to orthorhombic crystallographic structural phase transition well below room temperature, the resulting twin boundaries are inevitable. Therefore, one may attribute the resistive kink to a twin-boundary effect. In fact, in the presence of twin boundaries in Y123 crystals, the broader resistive shoulder which marks the onset of the twin-boundary pinning has been reported.[3,37] In this case, the FOT is suppressed by strong pinning by twin boundaries, and the phase transition temperature gives way to slightly higher twin-related pinning temperature.

Because the twin-boundaries act as directional pinning centers, the configuration between the field direction and twin-plane is important for the effect. Accordingly, if the twin boundary is involved in the resistive anomaly, the dependence of the kink temperature on the field orientation with respect to the twin-plane should show characteristic behavior, such as, a crossover from twin-boundary-pinning to the FOT as reported in Y123.[3] Therefore, the temperature dependence of the $ab$-plane resistivity $\rho_{ab}$ was also measured as a function of the angle $\theta$ between the $c$ axis and the field direction. The result in the $x=0.046$ crystal at $H=50$ kOe is shown in Fig. 4(b). The resistive anomaly, the abrupt change in the temperature dependence of $\rho_{ab}$ and the following sharp drop in $\rho_{ab}$ as temperature decreases, is seen in each $\rho_{ab}(T)$ curve, and the kink temperature smoothly increases to higher temperatures as $\theta$ increases, with no indication of crossover behavior. This angular dependence of the phase transition temperature will be discussed in detail in the Sec. IV B.

### C. Magnetic phase diagram

The characteristic fields and temperatures obtained from the magnetization ($M$-$H$) and resistivity ($\rho_{ab}$-$T$) measurements in the $x=0.046$ crystal are plotted in the $H$-$T$ phase diagram as shown in Fig. 5. In the resistivity measurements, the irreversibility temperature $T_{irr}$ has been defined with the resistivity criterion of $\rho_{ab}=2\times10^{-7}\Omega$ cm. The $H_{pt}(T)$ line from the $M$-$H$ results agree well with the $T_{pt}(H)$ line from the $\rho_{ab}$-$T$ results, strongly indicating that the $T_{pt}$ in the $\rho_{ab}$-$T$ measurements marks the vortex lattice phase transition. On the other hand, due to the different criterion, the $H_{irr}(T)$ line in the $M$-$H$ measurements is separated from the $T_{irr}(H)$ line in the $\rho_{ab}$-$T$ measurements.

For all samples studied, the phase transition lines $H_{pt}(T)$ are located well above the irreversibility lines $H_{irr}$(T). Although the $H_{irr}(T)$ line is dependent on the criterion and hence on the experimental condition, it can be regarded as a boundary around which the pinning of the vortex lattice sets in. Then, it follows that there are two phases such as a pinned lattice phase and an unpinned lattice phase in the vortex phase diagram below the $H_{pt}(T)$ lines. Existence of two such phases in the vortex lattice state has been recently demonstrated in Bi2212 system.[38] In this context, the vortex states in La214 are essentially identical with those in Bi2212.

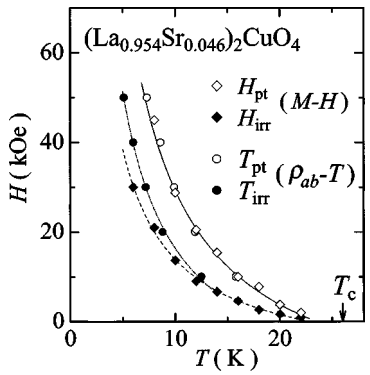


FIG. 5. The characteristic fields and temperatures obtained from the magnetization ($M$-$H$) and resistivity ($\rho_{ab}$-$T$) measurements in the $(La_{0.954}Sr_{0.046})_2CuO_4$ single crystal. Curves are the guides to the eye.

Now, we can draw the phase transition lines $H_{pt}(T)$ obtained for the three La214 crystals with different $x$ all together in the $H$-$T$ phase diagram as shown in Fig. 6, where $H_{pt}(T)$ lines reported for other HTSC materials, Y123 ($T_c=92.9$ K) (Ref. 5) and Bi2212 ($T_c=78.3$ K),[16] as well as a layered organic superconductor, $\kappa$-(BEDT-TTF)$_2$Cu[N(CN)$_2$]Br (BEDT; $T_c=11.3$ K),[39] have been included. The $H_{pt}(T)$ lines are found to shift toward higher fields as $x$ increases in La214. At first sight, this $x$ dependence in $H_{pt}(T)$ is thought to be attributable to an effect of $T_c$, because the present La214 samples range from underdoped ($x=0.046, 0.068$) to optimum doped ($x=0.077$), $T_c$ increasing with an increase of $x$. However, this upward trend of the $H_{pt}(T)$ lines with $T_c$ does not hold for the different material systems. On the contrary, the location of $H_{pt}(T)$ strongly depends on the specific material systems.

## IV. DISCUSSION

### A. Phase transition lines

The La214 system has shown basically the same magnetic and resistive signatures of the FOT which have been ob-

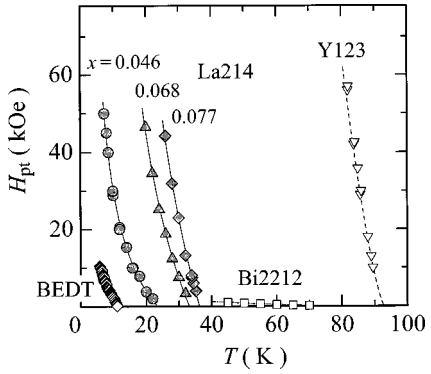


FIG. 6. The phase transition lines $H_{pt}(T)$ for La214 crystals with different Sr compositions. For comparison purposes, $H_{pt}(T)$ for Y123 (Ref. 5), Bi2212 (Ref. 16), and BEDT (Ref. 39) are included. Curves are the guides to the eye.

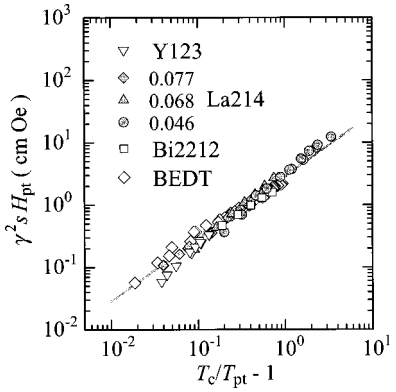


FIG. 7. Replot of the data in Fig. 6 in the universal scaling plot (Ref. 25); $\gamma^2 s H_{pt}$ vs $T_c/T-1$. From the scaling behavior, $H_{pt}(T)[\mathrm{Oe}]=2.85\gamma^{-2}s^{-1}(T_c/T-1)$ is obtained as a universal expression of the phase transition lines for layered superconductors.

served in the Y123 and Bi2212 systems. These results, in addition to the recent observation of the FOT in a layered organic superconductor,[39] imply that the FOT is a general phenomenon in the layered superconductors. We will, first of all, discuss the universal behavior found in the phase transition lines $H_{pt}(T)$, which may derive from the mechanism of the FOT common to all these materials.

As previously reported,[25] we found a universal scaling law for the FOT line. That is, all the transition lines for the HTSC materials (La214, Y123, and Bi2212) fall onto a single line when they were plotted as $\gamma^2 s H_{pt}$ vs $(T_c/T-1)$. It should be emphasized here that we have tried not to fit the obtained $H_{pt}(T)$ lines to theoretically proposed equations with several adjustable parameters; instead, we tried to find a phenomenological scaling law from the plots using the minimum number of parameters accessible by experiment. The resulting scaling behavior, shown in Fig. 7 where the data from Fig. 6 have been replotted, gives us a universal expression for the FOT lines in HTSC compounds:

$$H_{pt}(T)[\mathrm{Oe}]=2.85\gamma^{-2}s^{-1}(T_c/T-1). \quad (1)$$

Since the layered organic superconductor (BEDT) was reported to show the FOT, it would be interesting to see whether the universal scaling law works for BEDT as well. As seen in Fig. 7, the scaling, Eq. (1), works very well also for BEDT, further encouraging us to regard the FOT as a general phenomenon in the layered superconductors.

### B. Resistive phase transition

The normalization is applied for comparison purposes in such a way that the vertical resistivity axis is divided by the normal-state resistivity $\rho^N$ just above $T_c$ of each system. In Fig. 8, the resistivity curves for Y123,[4] La214 [Fig. 4(a)], and Bi2212 (Ref. 17) are reproduced in the order that the magnitude of anisotropy increases from left to right panels. Interestingly, the normalized resistivity values $\rho_{pt}/\rho^N$ where the anomalies are observed (indicated by the shaded area in Fig. 8) systematically decrease with increasing anisotropy factor: $\rho_{pt}/\rho^N > 10^{-1}\,\Omega$ cm in Y123, $\rho_{pt}/\rho^N = 10^{-1} \sim 10^{-2}\,\Omega$ cm in La214, and $\rho_{pt}/\rho^N = 10^{-4} \sim 10^{-6}\,\Omega$ cm in Bi2212, respectively. According to the Bardeen-Stephen model of flux-flow,[40] the resistivity in a magnetic field is given by $\rho(T,H)=\rho^N(T)\times H/H_{c2}(T)$, where $H_{c2}$ is the upper critical field. As shown in the inset in the middle panel of Fig. 8, the FOT in Y123 takes place at high $T/T_c$ (small $H_{c2}$) region with a high transition field $H_{pt}$, causing $\rho_{pt}/\rho^N \propto H_{pt}/H_{c2}$ to be larger. In Bi2212, the situation becomes the very opposite, and La214 is in between. Therefore, the systematic change of the phase transition fields with the anisotropy can be regarded as the origin of the behavior of $\rho_{pt}/\rho^N$ with respect to the anisotropy.

Next, we turn to the angular dependence of the $\rho_{ab}(T)$ curves. Figure 9 shows the phase transition temperature $T_{pt}$ in the La214 ($x=0.046$) crystal as a function of the angle $\theta$ between the field $H$ and the $c$ axis [data from Fig. 4(b)]. The $T_{pt}(\theta)$ increases monotonically as $\theta$ is increased, without the anomaly which is expected for the case when the twin-boundary-pinning is involved in the development of the resistive kink.[3] The reason why the twin boundary in La214 is not very effective as a strong directional pinning center will be rationalized as follows. According to TEM observations,[41] the separation of the twin boundaries in a La214 compound is of the order of $\sim 50$ Å. This indicates that the dimensions of twin planes are extremely small com-

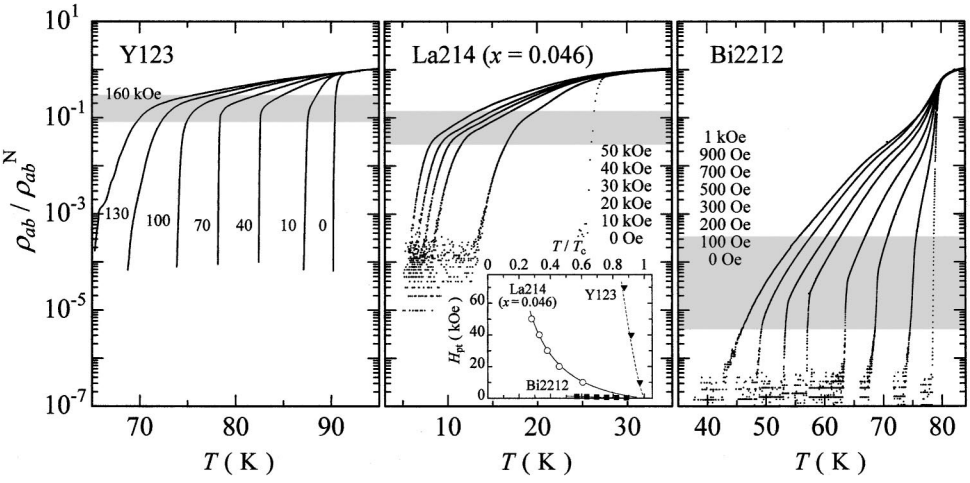


FIG. 8. Temperature dependence of the normalized $ab$-plane resistivity $\rho_{ab}/\rho_{ab}^N$ in Y123 (Ref. 4) (left), La214 ($x=0.046$) (middle), and Bi2212 (Ref. 17) (right) under various fields. $\rho_{ab}^N$ is the resistivity just above $T_c$. Inset: the FOT lines in the normalized phase diagram.

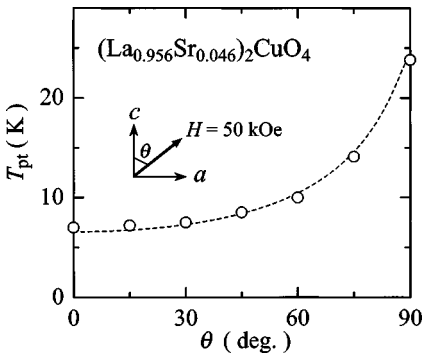


FIG. 9. Dependence of the phase transition temperature $T_{pt}(\theta)$ in the $(La_{0.954}Sr_{0.046})_2CuO_4$ single crystal on angle $\theta$ between the $c$ axis and the magnetic field ($H=50$ kOe). The dotted curve is a least-squares fit of $T_{pt}(\theta)$ by Eq. (2), providing the anisotropy parameter of $\gamma^2 = 2680$.

pared to the sample dimensions, implying that the twin planes do not extend over the sample thickness. This *microtwin* structure will not suit for a directional pinning site, likewise for a strong pinning source.

Following the angular scaling rules for anisotropic superconductors,[42] we can obtain the angular dependence of transition lines by the replacement of magnetic field $H$ with $H^*=\epsilon(\theta)H$, where $\epsilon(\theta)=(\gamma^{-2}\sin^2\theta+\cos^2\theta)^{1/2}$. Since we have Eq. (1) as a universal expression for the phase transition lines, the angular dependence of the phase transition temperature $T_{pt}(\theta)$ then reads

$$T_{pt}(\theta)=T_c/[\gamma^2 s\epsilon(\theta)H/2.85+1]. \tag{2}$$

The dotted curve shown in Fig. 9 is the least-squares fit of $T_{pt}(\theta)$ to Eq. (2). Using the experimentally determined values of $T_c=25.6$ K and $s=6.6$ Å, the fitting gives $\gamma^2=2680$. This value is in fair agreement with the value of 2900 determined from the anisotropic resistivity measurement. This analysis of the angular dependence of $T_{pt}$ proved to be quite useful in that (i) the twin boundary pinning as a source of resistive kink was ruled out, (ii) the validity of the universal scaling law [Eq. (1)] was demonstrated from a different aspect, and (iii) the value of $\rho_c/\rho_{ab}$ just above $T_c$ turned out to be a reasonable estimate of the anisotropy parameter $\gamma^2$ for the purpose of scaling.

### C. Magnetization jump and entropy change

The change of the thermodynamic quantities at the phase transition is important for understanding the mechanism of the phenomenon. In spite of the systematic and universal features found in the FOT, rather material specific behavior has so far been reported on the magnitude and temperature dependence of magnetization and entropy changes at the FOT. In Y123, the jump in the magnetization $\Delta M_{pt}$ at the FOT was a monotonous decreasing function of temperature, while the entropy change per pancake vortex $\Delta s_{pt}$ upon transition was almost temperature independent.[8,9] On the other hand, in Bi2212, $\Delta M_{pt}$ increased monotonically with temperature, reached a maximum at around 7 K below $T_c$, and then dropped rapidly on approaching $T_c$. As for $\Delta s_{pt}$ in Bi2212, the value seemed to diverge as temperature approached $T_c$.[13]

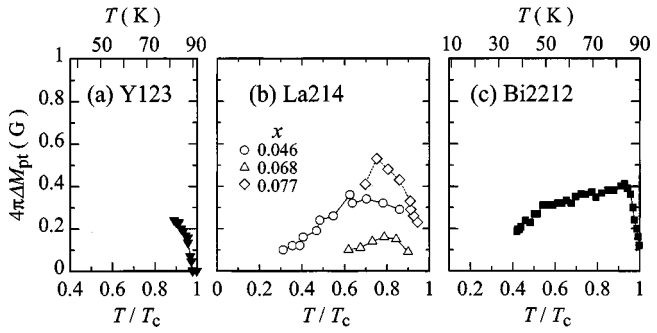


FIG. 10. Magnitude of magnetization jump $\Delta M_{pt}$ at the FOT as a function of the normalized temperature $T/T_c$ in (a) Y123 (Ref. 9), (b) La214, and (c) Bi2212 (Ref. 13). Normal temperature scale is also shown on the upper axes.

The present result for the temperature dependence of $\Delta M_{pt}$ for the three La214 crystals is plotted in Fig. 10(b). For comparison purposes, normalized temperature $T/T_c$ is used for the horizontal axis, and the reported data for Y123 (Ref. 9) and Bi2212 (Ref. 13) are also reproduced with the same temperature scale in Figs. 10(a) and 10(c), respectively. From the comparison of these three figures, it is found that the temperature dependence of $\Delta M_{pt}$ for all systems shows quite similar behavior. The $\Delta M_{pt}$ in La214 initially increases with temperature, reaches a maximum at around $T/T_c = 0.8$, and then drops as temperature approaches $T_c$. The whole feature also holds for Bi2212, while only the descending part can be observed in Y123 possibly because of the limited narrow temperature window ($T/T_c>0.8$). A plausible explanation for this drop in $\Delta M_{pt}$ on approaching $T_c$ has been recently given by a theoretical study based on the London model.[43]

According to the Clausius-Clapeyron relation, the entropy change $\Delta s_{pt}$ at the FOT is associated with $\Delta M_{pt}$ as

$$\Delta s_{pt}=-\frac{s\phi_0}{4\pi k_B}\frac{\Delta M_{pt}}{H_{pt}}\frac{dH_{pt}}{dT}, \tag{3}$$

where $k_B, \phi_0$, and $s$ are the Boltzmann constant, the flux quantum, and the distance between $CuO_2$ planes, respectively. Note that $\Delta s_{pt}$ gives, in a sense, the normalized entropy change, since $\Delta s_{pt}$ is in units of $k_B$ per pancake vortex. $\Delta s_{pt}$ evaluated using Eq. (3) as a function of the normalized temperature, $T/T_c$, for three La214 samples are plotted in Fig. 11(b). Again, the data for Y123 (Ref. 9) and Bi2212 (Ref. 13) are shown in Figs. 11(a) and 11(c), respectively. Estimated values of $\Delta s_{pt}$ for La214 at temperatures distant from $T_c$ are of the same order of magnitude ($\Delta s_{pt}=0.2-0.4k_B$) as determined in Y123 and Bi2212. This result reveals that the degrees of freedom contributing to the FOT are almost the same for all three materials, suggesting that the vortex fluid state in each high-$T_c$ superconductor is of the same nature. In contrast to the temperature dependence of $\Delta s_{pt}$ in Y123 which is nearly constant, that for La214 yields a similar behavior as in Bi2212; i.e., $\Delta s_{pt}$ increases monotonically with temperature to as large as $\Delta s_{pt}\sim 1.5k_B$ at temperatures close to $T_c$. These differences in the temperature dependence of $\Delta s_{pt}$ have not been understood properly, and should be subjected to future investigation.

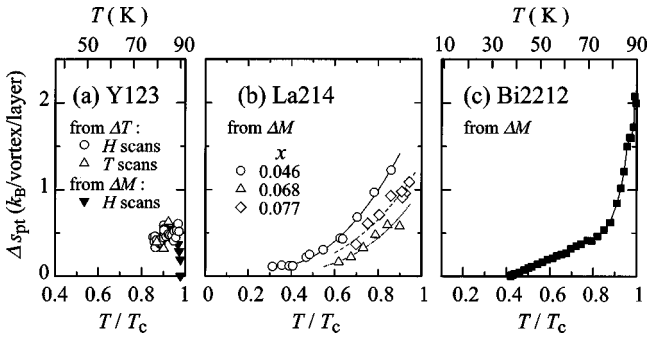


FIG. 11. Entropy change $\Delta s_{pt}$ at the FOT as a function of the normalized temperature $T/T_c$ in (a) Y123 (Ref. 9), (b) La214, and (c) Bi2212 (Ref. 13). Normal temperature scale is also shown on the upper axes.

## V. CONCLUSION

In $(La_{1-x}Sr_x)_2CuO_4$ (La214) single crystals ($0.046 \leqslant x \leqslant 0.077$), the first-order phase transition (FOT) of the vortex lattice was studied by means of magnetization and resistivity measurements. Both measurements show the same signatures of the FOT as have been reported in Y123 and Bi2212 compounds. Now that the FOT has been observed in all the well-studied prototype high temperature superconductors (HTSC; Y123, Bi2212, and La214), the FOT can be regarded as a general phenomenon in HTSC's.

The comparisons of the results in La214 with those in Y123 and Bi2212 were made with the help of normalization of scales. The findings from such comparisons included; (i) the normalized phase transition resistivity $\rho_{pt}/\rho^N$ systematically changed with respect to the anisotropy factor $\gamma^2$, (ii) the phase transition lines $H_{pt}(T)$ followed a scaling law [Eq. (1)], (iii) the magnetization change $\Delta M_{pt}$ at the FOT showed similar dependence on the normalized-temperature in La214, Y123, and Bi2212, and (iv) the magnitude of the entropy change per pancake vortex $\Delta s_{pt}$ at the phase transition was almost the same order of magnitude for the three HTSC systems.

These results indicate that the relevant parameters for the FOT are the anisotropy factor $\gamma^2$, the distance between superconducting layers $s$, and the critical temperature $T_c$. This will result from the fact that the phase transition is dominated by the properties of the pancake vortices. This, in turn, reflects the fact that all the HTSC materials are composed of $CuO_2$ planes of the same nature, but with different coupling constants determined by the superconducting-layer spacing and by the doping level. Therefore, it is tempting to think that the FOT is the transition of the vortex-lattice (solid) state to the pancake-vortex (gas) state.

## ACKNOWLEDGMENTS

We would like to thank J. Clem, A. E. Koshelev, and T. Tamegai for fruitful discussions. This work was, in part, supported by the Core Research for Evolutional Science and Technology (CREST) of the Japan Science and Technology (JST) Corporation and by the Original Industrial Technology R&D Promotion Program from the New Energy and Industrial Technology Development Organization (NEDO) of Japan. One of the authors (T.S.) would like to thank the Japan Society for the Promotion of Science (JSPS) for financial support.

[1] For reviews, D.J. Bishop *et al.*, Science **255**, 165 (1992); D.A. Huse *et al.*, Nature (London) **358**, 553 (1992); G. Blatter *et al.*, Rev. Mod. Phys. **66**, 1125 (1994); G.W. Crabtree and D.R. Nelson, Phys. Today **50**(4), 38 (1997).
[2] H. Safar *et al.*, Phys. Rev. Lett. **69**, 824 (1992); W.K. Kwok *et al.*, *ibid.* **72**, 1092 (1994).
[3] W.K. Kwok *et al.*, Phys. Rev. Lett. **69**, 3370 (1992).
[4] H. Safar *et al.*, Phys. Rev. Lett. **70**, 3800 (1993).
[5] U. Welp *et al.*, Phys. Rev. Lett. **76**, 4809 (1996).
[6] R. Liang *et al.*, Phys. Rev. Lett. **76**, 835 (1996).
[7] T. Nishizaki *et al.*, Phys. Rev. B **53**, 82 (1996).
[8] M. Willemin *et al.*, Phys. Rev. Lett. **81**, 4236 (1998).
[9] A. Schilling *et al.*, Nature (London) **382**, 791 (1996); A. Schilling *et al.*, Phys. Rev. Lett. **78**, 4833 (1997).
[10] M. Roulin *et al.*, Phys. Rev. Lett. **80**, 1722 (1998).
[11] M. Roulin *et al.*, Science **273**, 1210 (1996).
[12] H. Pastoriza *et al.*, Phys. Rev. Lett. **72**, 2951 (1994).
[13] E. Zeldov *et al.*, Nature (London) **375**, 373 (1995).
[14] B. Khaykovich *et al.*, Phys. Rev. Lett. **76**, 2555 (1996); Y. Yamaguchi *et al.*, in *Advances in Superconductivity VIII*, edited by H. Hayakawa and Y. Enomoto (Springer-Verlag, Berlin, 1996), p. 209.
[15] T. Hanaguri *et al.*, Physica C **256**, 111 (1996).
[16] S. Watauchi *et al.* Physica C **259**, 373 (1996).
[17] T. Sasagawa *et al.* (unpublished).
[18] D.T. Fuchs *et al.*, Phys. Rev. B **55**, R6156 (1997).
[19] N. Morozov *et al.*, Phys. Rev. B **54**, R3784 (1996).
[20] R.A. Doyle *et al.*, Phys. Rev. Lett. **75**, 4520 (1995).
[21] Y. Ando *et al.*, Phys. Rev. B **52**, 3765 (1995).
[22] J. Shimoyama *et al.*, Physica C **282-287**, 2055 (1997).
[23] A. Houghton *et al.*, Phys. Rev. B **40**, 6763 (1989); E.H. Brandt, Phys. Rev. Lett. **63**, 1106 (1989); G. Blatter and B.I. Ivlev, Phys. Rev. B **50**, 10 272 (1994).
[24] L.I. Glazman and A.E. Koshelev, Phys. Rev. B **43**, 2835 (1991); L.L. Daemen *et al.*, Phys. Rev. Lett. **70**, 1167 (1993); Phys. Rev. B **47**, 11 291 (1993); R. Ikeda, J. Phys. Soc. Jpn. **64**, 1683 (1995).
[25] T. Sasagawa *et al.*, Phys. Rev. Lett. **80**, 4297 (1998).
[26] T. Naito *et al.*, Czech. J. Phys. **46**, 1585 (1996).
[27] T.T.M. Palstra *et al.*, Phys. Rev. B **41**, 6621 (1990); T. Shibauchi *et al.*, Phys. Rev. Lett. **72**, 2263 (1994); T. Kimura *et al.*, in *Advances in Superconductivity VII*, edited by K. Yamafuji and T. Morishita (Springer-Verlag, Berlin, 1995), p. 539.
[28] T. Kimura *et al.*, Physica C **192**, 247 (1992).
[29] M. Willemin *et al.*, Phys. Rev. B **59**, R717 (1999).
[30] D.E. Farrell *et al.*, Phys. Rev. Lett. **61**, 2805 (1988); D.E. Farrell *et al.*, *ibid.* **64**, 1573 (1990); K. Takenaka *et al.*, Phys. Rev. B **50**, 6534 (1994).
[31] D.E. Farrell *et al.*, Phys. Rev. Lett. **63**, 782 (1989); J.C. Martinez *et al.*, *ibid.* **69**, 2276 (1992); Y. Kotaka *et al.*, Physica C **235-240**, 1529 (1994).
[32] P.G. de Gennes, *Superconductivity of Metals and Alloys* (Benjamin, New York, 1966).

[33] L.N. Bulaevskii *et al.*, Phys. Rev. Lett. **68**, 3773 (1992); V.G. Kogan *et al.*, *ibid.* **70**, 1870 (1993).
[34] T. Sasagawa *et al.*, J. Low Temp. Phys. **105**, 1201 (1996); M. Okuya *et al.*, Physica C **271**, 265 (1996).
[35] T. Nishizaki *et al.*, Phys. Rev. B **58**, 11 169 (1998); T. Nishizaki *et al.*, Physica C **282-287**, 2117 (1997).
[36] K. Deligiannis *et al.*, Phys. Rev. Lett. **79**, 2121 (1997).
[37] W.K. Kwok *et al.*, Phys. Rev. Lett. **64**, 966 (1990); W.K. Kwok *et al.*, *ibid.* **72**, 1088 (1994).
[38] D.T. Fuchs *et al.*, Phys. Rev. Lett. **80**, 4971 (1998); D.T. Fuchs *et al.*, Nature (London) **391**, 373 (1998).
[39] T. Shibauchi *et al.*, Phys. Rev. B **57**, R5622 (1998).
[40] J. Bardeen and M.J. Stephen, Phys. Rev. **140**, A1197 (1965).
[41] C.H. Chen *et al.*, Physica C **183**, 121 (1991).
[42] G. Blatter *et al.*, Phys. Rev. Lett. **68**, 875 (1992); R.G. Beck *et al.*, *ibid.* **68**, 1594 (1992).
[43] M.J.W. Dodgson *et al.*, Phys. Rev. Lett. **80**, 837 (1998).